

# Effect of nano-CeO<sub>2</sub> on microstructure properties of TiC/TiN+TiCN-reinforced composite coating

LI JIANING\*, CHEN CHUANZHONG and ZHANG CUIFANG

Key Laboratory for Liquid–Solid Structural Evolution and Processing of Materials (Ministry of Education),  
Department of Materials Science, Shandong University, Jinan' 250061, China

MS received 8 April 2011; revised 1 August 2011

**Abstract.** TiC/TiN+TiCN-reinforced composite coatings were fabricated on Ti–6Al–4V alloy by laser cladding, which improved surface performance of the substrate. Nano-CeO<sub>2</sub> was able to suppress crystallization and growth of crystals in the laser-cladded coating to a certain extent. With the addition of proper content of nano-CeO<sub>2</sub>, this coating exhibited fine microstructure. In this study, Al<sub>3</sub>Ti+TiC/TiN+nano-CeO<sub>2</sub> laser-cladded coatings have been studied by means of X-ray diffraction and scanning electron microscope. X-ray diffraction results indicated that Al<sub>3</sub>Ti+TiC/TiN+nano-CeO<sub>2</sub> laser-cladded coating consisted of Ti<sub>3</sub>Al, TiC, TiN, Ti<sub>2</sub>Al<sub>20</sub>Ce, TiC<sub>0.3</sub>N<sub>0.7</sub>, Ce(CN)<sub>3</sub> and CeO<sub>2</sub>, this phase constituent was beneficial in increasing microhardness and wear resistance of Ti–6Al–6V alloy.

**Keywords.** Rare-earth compounds; surface modification; laser cladding; microstructure; X-ray diffraction; intermetallic compounds.

## 1. Introduction

Laser cladding is an advanced surface modification technology that uses a high-power laser beam to form a composite coating with specific quality and low dilution that is metallurgically bonded to the substrate, which can greatly improve wear resistance of the substrate (Dutta Majumdar *et al* 2000, 2009; Wang *et al* 2010). TiC and TiN showed excellent properties of low density and wear resistance, etc (Wang *et al* 2007). During laser cladding process, TiC can react with TiN leading to the formation of titanium carbonitride (TiCN), which showed superior mechanical properties, such as low friction, high hardness (2500–3000 HV), high melting point (3050 °C) and enhanced wear resistance (Forn *et al* 2001).

Laser cladding of Al<sub>3</sub>Ti+TiC/TiN pre-placed powders on Ti–6Al–4V alloy formed TiC/TiN+TiCN-reinforced Al<sub>3</sub>Ti/Ti<sub>3</sub>Al matrix composite coating, which can greatly improve surface performance of the substrate. It was known that titanium aluminides display much better performance such as low density, high specific strength, elastic modulus, wear resistance and better mechanical behaviour with increase in temperature (Hisashi *et al* 2008). In addition, cerium as rare-earth elements (RE), has been applied successfully in many fields. An area of current interest is the modification of RE for application in surface engineering.

Investigation by Baligidad and Khaple (2009) indicated that Ce was able to refine the microstructure of laser-cladded coatings and also improved strength and ductility of the coatings. Furthermore, in the field of surface engineering, nano-materials have been used in research on laser cladding and laser surface alloys, which have many excellent properties such as strong acoustic, electric, magnetic and thermodynamic characteristics because of their quantum size and surface effect (Zeng *et al* 2002). Moreover, if amorphous layer is desired, then CeO<sub>2</sub> should dissolve, depress the fusion/eutectic temperature, stabilize the melt and retain glassy layer after laser cladding. Through the experiment, it was found that CeO<sub>2</sub> particles were easily reunited because of surface effect. Agglomeration of CeO<sub>2</sub> particles generally occurred on the grain boundaries, which were able to suppress the crystallization and growth of TiN/TiC precipitates to a certain extent.

Our present study investigates the microstructure and wear resistance of Al<sub>3</sub>Ti+TiC/TiN laser-cladded coatings with or without CeO<sub>2</sub>.

## 2. Experimental

Cross-flow CO<sub>2</sub> laser cladding equipment was used in this experiment. Main components of the laser cladding equipment were: CO<sub>2</sub> laser device (maximum power, 1.5 kW and it could be adjusted continuously), optical system, working table and operation system. It should be mentioned that too high power can burn out a portion of the

\*Author for correspondence (jn2369@163.com)

**Table 1.** Parameters and materials of laser-cladding process in experiment.

Number	Substrate material	Powders composition (wt%)	Laser power (W)	Scanning speed (mm·s <sup>-1</sup> )	Spot diameter (mm)
Sample 1	Ti-6Al-4V alloy	Al <sub>3</sub> Ti-20TiC-35TiN	850–1000	2–6	4
Sample 2		Al <sub>3</sub> Ti-20TiC-20TiN			
Sample 3		Al <sub>3</sub> Ti-20TiC-20TiN-1.5CeO <sub>2</sub>			

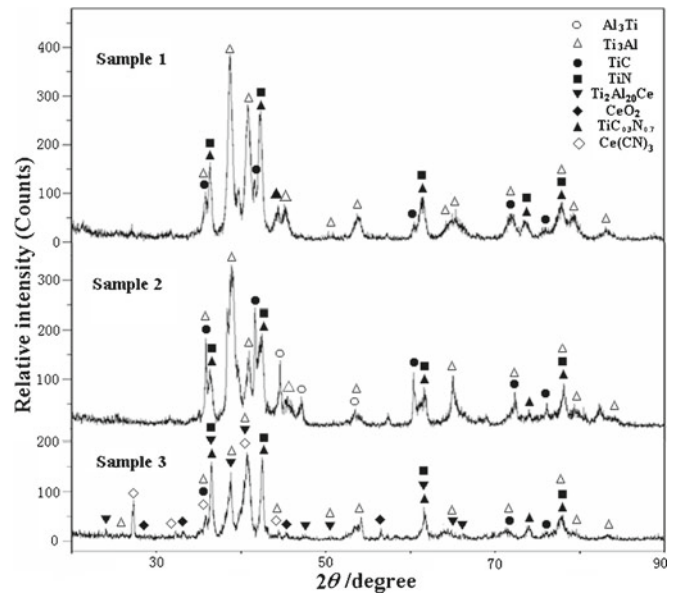
pre-placed powders, which can greatly influence quality of the coatings. Conversely, the laser power decided the inter-diffusion of substrate material into the cladded material, and the laser surface alloying cannot occur completely with too low power. Hence, in this study, the power was in the range of 850–1000 W.

The materials used for laser cladding in this experiment were Ti-6Al-4V alloy and powders of Al<sub>3</sub>Ti ( $\geq 99.5\%$  purity, 50–150  $\mu\text{m}$ ), TiC ( $\geq 99.5\%$  purity, 50–150  $\mu\text{m}$ ), TiN ( $\geq 99.5\%$  purity, 50–150  $\mu\text{m}$ ) and CeO<sub>2</sub> ( $\geq 99.5\%$  purity, 10–200 nm). The size of the samples of Ti-6Al-4V alloy was 10 × 10 × 10 mm. Thickness of the pre-placed layer was 0.6–0.8 mm, three-track lap coating was formed on samples and the lap rate was  $\sim 30\%$ . To protect the molten pool from oxidation, during laser cladding process, the coating surface was protected by an inert gas (Ar) with a flow rate of 30 L/min. The parameters and materials used in this experiment are shown in table 1.

According to the report by Zhao *et al* (2000), it was known that excessive rare-earth oxide can form many inclusions, which would markedly reduce a wear resistance of the composite coatings. On the other hand, we also found that an obvious improvement in wear resistance of Al<sub>3</sub>Ti+TiC/TiN laser-cladded coating was not achieved with too little CeO<sub>2</sub> content. Hence, 1.5 wt% nano-CeO<sub>2</sub> was used in this study.

MM200 disc wear tester was used to test wear resistance of the laser-cladded coatings, the rotational speed of the wear tester was 400 r/min, and the load was 5 kg. The wear mass loss increased proportionally on prolonging, friction time. The honing wheel was composed of quenching and tempering steels (W18Cr4V).

The samples were polished and etched in a hydrofluoric acid and nitric acid aqueous solution. The volume ratio of hydrofluoric acid and nitric acid aqueous solution was 1:2:3 which revealed growth morphology of the compounds in the laser-cladded coatings. DMAX/2500PCX X-ray diffraction (XRD) was used to determine the phase constituents of these composite coatings. The microstructure morphologies of the composite coatings were analysed by means of QUANTA200 scanning electron microscope (SEM). Element distributions of the composite coatings were measured using JXA-880R electron probe micro analyser (EPMA). HV-1000 microsclemeter was used to test the microhardness distributions of the composite coatings.

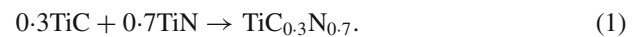
**Figure 1.** XRD diagrams of coatings in samples 1, 2 and 3.

### 3. Results and analysis

#### 3.1 XRD analysis

The overlap of XRD patterns of the composite coating in samples 1, 2 and 3 illustrated a significant phase evolution after laser cladding. As shown in figure 1, it was inferred that the phase area of the coating surface in sample 1 consisted of Ti<sub>3</sub>Al, TiC, TiN and TiC<sub>0.3</sub>N<sub>0.7</sub> and matrix of the coating mainly consisted of Ti<sub>3</sub>Al.

It was noticed that TiC<sub>0.3</sub>N<sub>0.7</sub> was produced in the coating due to the reaction between a portion of TiC and TiN, the reaction was described as follows:



Moreover, it was also found that the only Ti<sub>3</sub>Al diffraction peak was present in XRD pattern of sample 1. It should be considered that during the cladding process, a portion of TiN dissolved to deliver an amount of Ti into the molten pool, so a Ti-rich molten pool was produced. Therefore, Al<sub>3</sub>Ti can further react with Ti in molten pool leading to production of Ti<sub>3</sub>Al.

XRD result of the coating in sample 2 indicated that with decrease in TiN content, TiC diffraction peak increased significantly. It was known that the melting point of TiC (3150 °C) was higher than that of TiN (2950 °C), so it can be deduced that during the freezing time, TiC precipitated earlier than TiN. Thus, TiC was the nucleus in the precipitation and TiN precipitated around it. It was reasonable that with the decrease of the mass fraction of TiN pre-place powder, the content of TiN precipitates around TiC also decreased, thus resulting in the enhancement of TiC diffraction. On the other hand, according to (1), with the decrease of TiN, the production of TiC<sub>0.3</sub>N<sub>0.7</sub> consumed less TiC leading to high TiC diffraction peak and low diffraction peak of TiC<sub>0.3</sub>N<sub>0.7</sub>.

With the addition of nano-CeO<sub>2</sub>, there were Ti<sub>3</sub>Al, TiC, TiN, Ti<sub>2</sub>Al<sub>20</sub>Ce, TiC<sub>0.3</sub>N<sub>0.7</sub>, Ce(CN)<sub>3</sub> and CeO<sub>2</sub> in the coating of sample 3. Ti<sub>2</sub>Al<sub>20</sub>Ce was produced due to the reaction

between Al<sub>3</sub>Ti and nano-CeO<sub>2</sub> particles. It should be considered that the production of Ti<sub>2</sub>Al<sub>20</sub>Ce consumed a large amount of Al in the molten pool. Hence, with the decrease of Al, a Ti-rich molten pool was achieved leading to the disappearance of Al<sub>3</sub>Ti. According to the report by Tian *et al* (2006), during the cladding process, a portion of CeO<sub>2</sub> was decomposed as follows:



Then, Ce was able to further react with TiC/TiN leading to the formation of Ce(CN)<sub>3</sub> and Ti particles. Though the experiment progressed under the protection of the inert gas, carbides/nitrides were not stable at higher temperatures in presence of oxygen, and some of it was converted to oxide that also lead to off-stoichiometry and decrease of TiN/TiC. However, due to the short solidification time and surface treatment of the samples, this influence on the laser-cladded coatings was not serious.

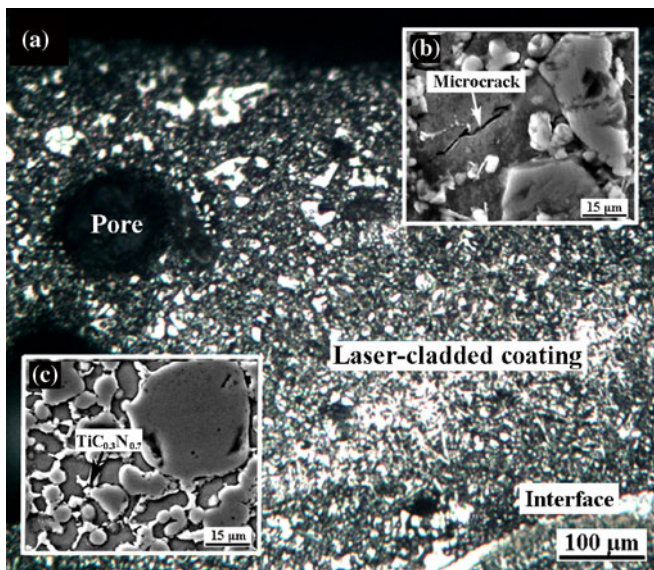


**Figure 2.** Microstructure of coating in sample 1. (a) Cross-sectional view with low magnification, (b) un-melted TiC/TiN block and microcrack and (c) TiC<sub>0.3</sub>N<sub>0.7</sub>.

### 3.2 Microstructure

**3.2a Microstructure of Al<sub>3</sub>Ti+TiC/TiN laser-cladded coatings:** Figure 2 shows microstructure of the overview cross-section of the laser-cladded coating in sample 1. It was noted that there are pores and cracks in this coating. In fact, dilution rate of the substrate to the coating decreased with the increase of TiC/TiN content, which lead to the energy of the laser beam that transmitted onto Ti-6Al-4V substrate to decrease. Therefore, the freezing time of the molten pool was short, and the steam did not have enough time to escape leading to the formation of the pores.

On the other hand, due to high TiC/TiN content, thermal stress of the laser-cladded coating in sample 1 was greater than the material yield strength limit, thus resulting in the production of the microcrack (see figure 2b). Combining the XRD results, an amount of TiC<sub>0.3</sub>N<sub>0.7</sub> was produced in the coating (see figure 2c), which was a solid solution of *fcc* TiN and *fcc* TiC incorporating advantages and characteristics of both TiN and TiC (Ertuerk *et al* 1991).

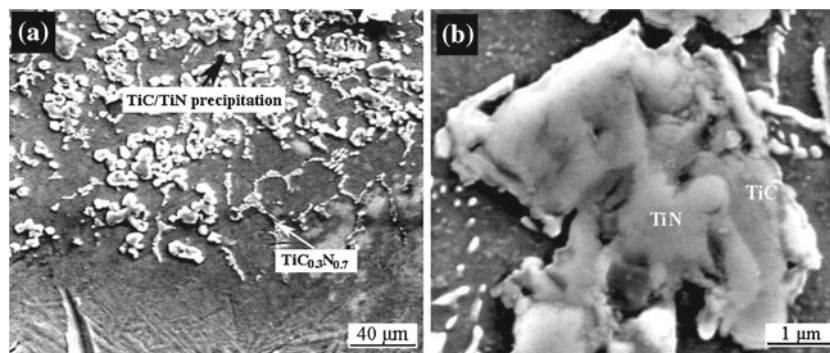


**Figure 3.** SEM micrographs of coating in sample 2. (a) Interface and (b) TiC/TiN precipitates.



As shown in figure 3(a), it is noted that there was a metallurgical combination between the coating in sample 2 and Ti-6Al-4V alloy substrate. During the cladding process,  $\text{TiC}_{0.3}\text{N}_{0.7}$ , TiC and TiN particles acted as dendrite nuclei, which were dispersed in the molten pool. Furthermore, the larger depth of laser melting pool and the rapid convection by a high energy density lead the distribution of  $\text{TiC}_{0.3}\text{N}_{0.7}$  precipitates to a deeper depth. Because the density of  $\text{TiC}_{0.3}\text{N}_{0.7}$  was larger than that of TiC/TiN (Yang *et al* 2010). As shown in figure 3(b), it is noted that bulk-shape precipitates were present in the clad zone. Nevertheless, its surface was not smooth, and there were protuberant block-shape precipitations adjacent to it. As mentioned earlier protuberant precipitation consisted of TiN and the bulk-shape precipitation below it was TiC.

**3.2b Microstructure of  $\text{Al}_3\text{Ti}+\text{TiC}/\text{TiN}+\text{nano-CeO}_2$  laser-cladded coating:** Figure 4(a) shows that fine TiC/TiN precipitates were dispersed in the coating. Furthermore, there were also some nano- $\text{CeO}_2$  particles dispersed in the coating, and uniform distribution of nano- $\text{CeO}_2$  particles was advantageous to improve the hardness and wear resistance of the coatings. On the other hand, as mentioned earlier, a portion of  $\text{CeO}_2$  was decomposed into Ce and  $\text{O}_2$  during the cladding process. Investigation by Li *et al* (2008) indicated that Ce was able to refine the microstructure coatings and reduced the secondary dendrite spacing. Thus, the composite coating in sample 3 showed finer microstructure than that of the coating in sample 2.

Moreover, combining the XRD results,  $\text{Ce}(\text{CN})_3$  metal cyanide was produced in this coating (see figure 4b). Lai *et al* (1993) reported that the production of the metal cyanide can further enhance microhardness of the composite coating.

In addition, once the molten layer was formed, the dispersoids dissolved partially or fully, and hence, nano- $\text{CeO}_2$  can neither remain  $\text{CeO}_2$  nor nano-metric in size. However, energy distribution of the laser beam was uneven. Thus, a portion of nano- $\text{CeO}_2$  particles in the edge of the facula were able to retain the nano-metric size, which diffused into every portion of the molten pool due to their high diffusion coefficient (Zhang *et al* 2008). Then, these nano- $\text{CeO}_2$  particles acted as nucleation sites during the solidification process, which was beneficial in refining the microstructure of the coating. Combining XRD results, the enwrapped-like  $\text{Ti}_2\text{Al}_{20}\text{Ce}$  phase was formed in the coating of sample 3, and then increased in size via incomplete peritectic reaction (Zhao *et al* 2010). In addition, it was noted that agglomeration of nano- $\text{CeO}_2$  particles occurred in the coating (see figure 4c), this indicated that nano- $\text{CeO}_2$  particles were easily reunited because of the surface effect, which suppressed the crystallization and growth of  $\text{Ti}_2\text{Al}_{20}\text{Ce}$  crystal.

Stepanova *et al* (2000) reported that usually TiCN is added to the melt as a tablet sintered with a metal activator, changing the addition interaction with the liquid alloy. As mentioned above, Ce was able to prevent the growth of  $\text{TiC}_{0.3}\text{N}_{0.7}$  crystal. Thus,  $\text{TiC}_{0.3}\text{N}_{0.7}$  exhibited a fine microstructure (see figure 4d). Production of carbonitrides provided

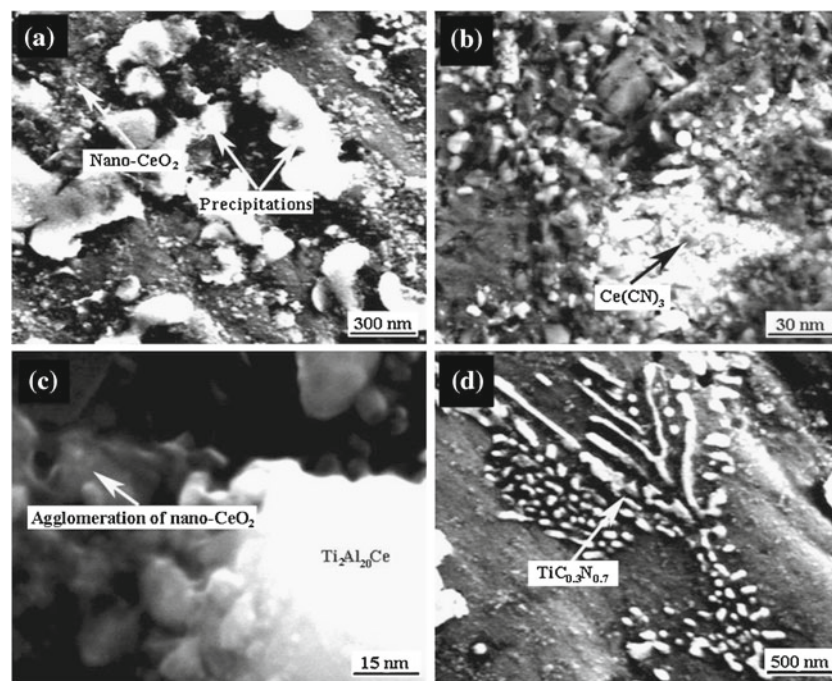


**Figure 4.** SEM micrographs of composite coating in sample 3. (a) Clad zone, (b) nano- $\text{CeO}_2$  and  $\text{Ce}(\text{CN})_3$ , (c) agglomeration of nano- $\text{CeO}_2$  and (d)  $\text{TiC}_{0.3}\text{N}_{0.7}$ .

hardening and wear resistance to the composite coating. Investigation by Shen *et al* (1997) revealed that nano-CeO<sub>2</sub> prevented the defects in the coating and improved quality of the surface. Grain boundary was also purified by cerium concentration. Thus, crack tendency of the coatings decreased. Furthermore, it should be considered that during laser-cladding process, CeO<sub>2</sub> absorbed some energy from the laser beam, which could decrease the existing time of the molten pool and also accelerate the super-cooling degree. Thus, the diffusibility of the particles in this molten pool was prevented to a certain extent.

### 3.3 Microhardness distribution and wear resistance

Microhardness as a function of depth from the coating surface to Ti-6Al-4V substrate is shown in figure 5. It can be seen that microhardness of coating in sample 1 was in the range of 1100–1250 HV<sub>0.2</sub> due to the action of hard phase Ti<sub>3</sub>Al+TiC/TiN+TiC<sub>0.3</sub>N<sub>0.7</sub>. Furthermore, it was noted that microhardness of the coating in sample 2 was in the range of 1200–1350 HV<sub>0.2</sub>, which was higher than that of sample 1 due to the massive dilution of TiC/TiN primary particles.

It was also noticed that with the addition of nano-CeO<sub>2</sub>, microhardness of the coating in sample 3 was higher than that of sample 2 (see figure 6). Enhancement of microhardness of the coating in sample 3 can be ascribed to the actions of Ce(CN)<sub>3</sub>, CeO<sub>2</sub>, Ti<sub>2</sub>Al<sub>20</sub>Ce phases and fine grain strengthening.

When the load was 5 kg, wear test result revealed that wear-volume loss of the substrate was ~2 times higher than that of the coating in sample 2. However, wear-volume loss of the coating in sample 3 was ~4.5–5 times lesser than that of the substrate (see figure 7). It was considered that due to higher microhardness, the coating in sample 3 exhibited better wear resistance than

that of the coating in sample 2. Moreover, it should be mentioned that the coating in sample 1 showed poor wear resistance mainly due to poor quality of the microstructure.

SEM micrographs showed that when the load was 5 kg, deep peeled holes and microcrack were produced in the coating surface of sample 2 (see figure 8). Nevertheless, the coating surface in sample 3 showed shallow grooves free of dip hole and microcrack. As mentioned previously, Ce was able to improve the strength and ductility of the coatings. Thus, due to the action of the wear plate, dip peeled holes and microcracks were not present in the coating surface of sample 3.

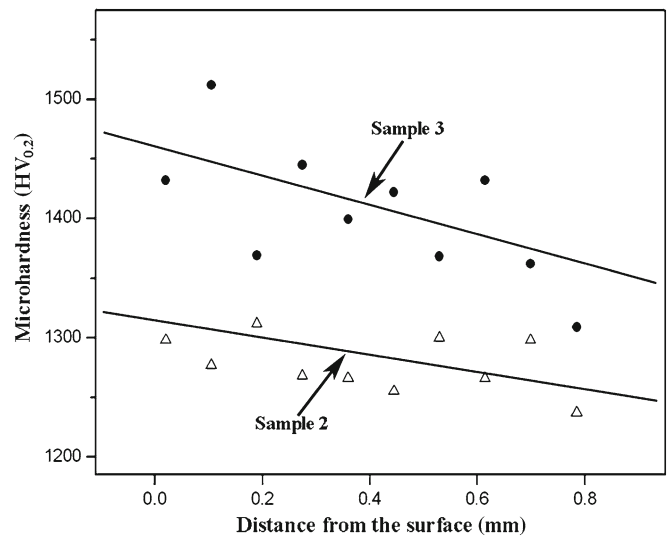


**Figure 6.** Microhardness distribution of coatings in samples 2 and 3.

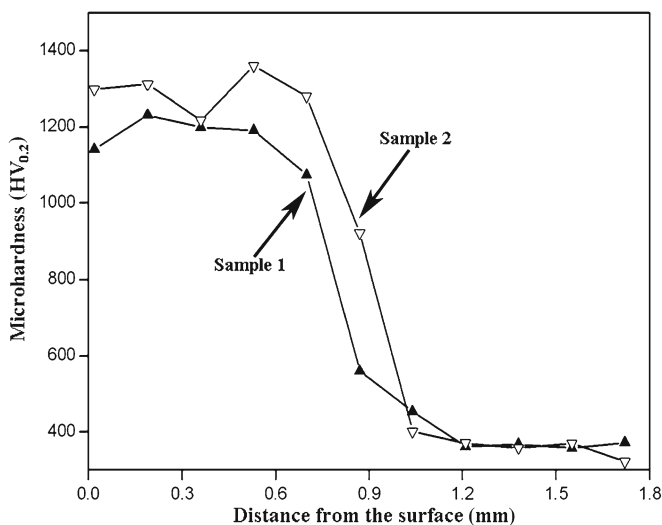


**Figure 5.** Microhardness distribution of coatings in samples 1 and 2.

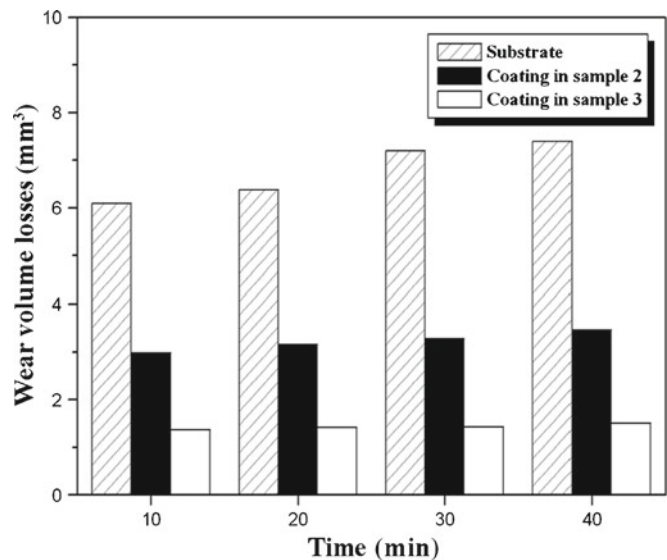


**Figure 7.** Wear mass losses of composite coatings in samples 2, 3 and Ti-6Al-4V alloy.

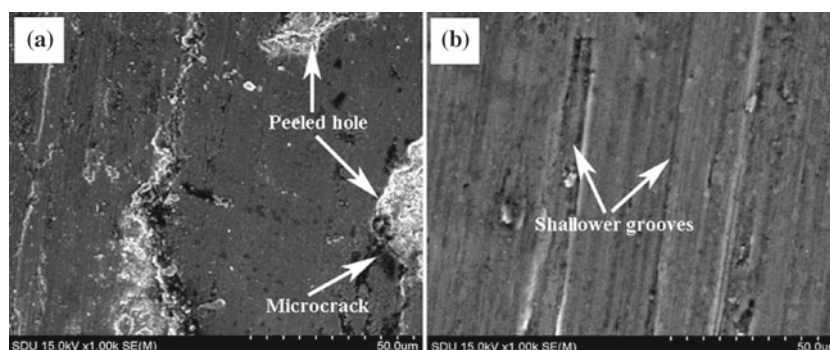


**Figure 8.** Worn morphologies of coating surface (a) in sample 2 and (b) in sample 3.

#### 4. Conclusions

Laser cladding of  $\text{Al}_3\text{Ti}+\text{TiC}/\text{TiN}$  pre-placed powders on Ti-6Al-4V alloy can form a  $\text{TiC}/\text{TiN}+\text{TiCN}$  reinforced composite coating, which improves wear resistance of Ti-6Al-4V alloy.  $\text{Ti}_3\text{Al}$  or  $\text{Ti}_3\text{Al}/\text{Al}_3\text{Ti}$ ,  $\text{TiC}$ ,  $\text{TiN}$  and  $\text{TiC}_{0.3}\text{N}_{0.7}$  were the pre-placed powders used in  $\text{Al}_3\text{Ti}+\text{TiC}/\text{TiN}$  laser-cladded coating. Nano- $\text{CeO}_2$  can suppress the crystallization and growth of the precipitates to a certain extent, resulting in fine microstructure. With addition of proper content of nano- $\text{CeO}_2$ , microhardness and wear resistance of  $\text{Al}_3\text{Ti}+\text{TiC}/\text{TiN}$  laser-cladded coating were significantly improved due to the action of  $\text{Ce}(\text{CN})_3/\text{CeO}_2/\text{Ti}_2\text{Al}_{20}\text{Ce}$  phases and high quality microstructure. Wear-volume loss of  $\text{Al}_3\text{Ti}+\text{TiC}/\text{TiN}+\text{nano-CeO}_2$  laser-cladded coating was  $\sim 4.5$ –5 times lesser than that of Ti-6Al-4V alloy.

#### Acknowledgements

This work was supported by the Development Project of Science and Technology of Shandong Province (2006GG2204010) and Independent Innovation Foundation of Shandong University, IIFSDU (31370070613156).

#### References

Baligidad R G and Khaple S 2009 *Bull. Mater. Sci.* **32** 531

- Dutta Majumdar J, Manna I, Kumar A, Bhargava P and Nath A K 2009 *J. Mater. Process. Technol.* **209** 2237
- Dutta Majumdar J, Mordike B L and Manna I 2000 *Wear* **242** 18
- Ertuerk E, Knotek O, Bergmer W and Prengel H-G 1991 *Surf. Coat. Technol.* **46** 39
- Forn A, Picas J A, Fuentes G G and Elizalde E 2001 *Int. J. Refract. Met. Hard Mater.* **19** 507
- Hisashi S, Takashi M, Toshiyuki F, Susumu O, Yoshimi W and Masaharu K 2008 *Acta Mater.* **56** 4549
- Lai F D, Wu T I and Wu J K 1993 *Surf. Coat. Technol.* **58** 79
- Li M X, Zhang S H, Li H S, He Y Z, Yoon J H and Cho T Y 2008 *J. Mater. Process. Technol.* **202** 107
- Shen Y F, Chen J Z, Feng Z C and Liang Y 1997 *J. Chinese Rare-Earth Soc.* **15** 344
- Stepanova N N, Rodionov D P, Sazonova V A and Khlystov E N 2000 *Mater. Sci. Eng.* **A284** 88
- Tian Y S, Chen C Z, Chen L X and Huo Q H 2006 *Scr. Mater.* **54** 847
- Wang J, Li Y J and Gerasimov S A 2007 *Bull. Mater. Sci.* **30** 415
- Wang X H, Zhang M and Qu S Y 2010 *Opt. Laser Technol.* **48** 893
- Yang Y L, Yao W M and Zhang H Z 2010 *Surf. Coat. Technol.* **205** 620
- Zeng Y, Lee S W, Gao L and Ding C X 2002 *J. Eur. Ceram. Soc.* **22** 347
- Zhang S H, Li M X, Cho T Y, Yoon J H, Lee C G and He Y Z 2008 *Opt. Laser Technol.* **40** 716
- Zhao H L, Song Y, Li M and Guan S K 2010 *J. Alloys Compd.* **508** 206
- Zhao T, Xun C, Wang S X and Zheng S A 2000 *Thin Solid Films* **379** 128